Quantum Chemical Study of Some Benzimidazole and its Derivatives as Corrosion Inhibitors of Steel in HCl Solution

Shuangkou Chen[1], Bai He[1], Yuanzhi Liu[2], Yue Wang[1], Jianfang Zhu[1]*

[1]College of Chemistry and Chem-engineering, Chongqing University of Science and Technology, Chongqing 401331, China;
[2]Zhongyuan Oilfield Company Gas Processing Plant,Puyang 457061,China
*E-mail: cskcn@yeah.net

The relationships between corrosion inhibition performance of three kinds of benzimidazole inhibitors compounds and their molecular electronic properties have been investigated using quantum chemistry method. Quantum parameters such as highest occupied molecular orbital (HOMO), lowest unoccupied molecular orbital (LUMO), energy gap between HOMO & LUMO and Mulliken charges have been calculated at the level of DFT/B3LYP with various basic sets 6-31+G(d), 6-31+G(d,p) and 6-311+G(d,p). Quantum calculation results were discussed by using linear regression analysis method which found inhibition efficiency had a good linear relationship with HOMO energy, energy gap and total charge of substituent group R3. Among three basic sets, 6-311+G(d,p) can provide more accurate calculation results. It was found the theoretical data were well accorded with reported experimental results. Finally, the study may be helpful to design and discover some new homologous inhibitors with good performance.
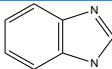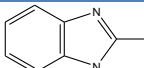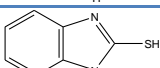
1. INTRODUCTION

To protect metal surface against corrosion, an effective method is to reasonably apply corrosion inhibitors in acid medium [1-3]. Nowadays corrosion inhibitors, as a protection technique, are widely used in petroleum, chemical industry, construction and so on. Some organic molecules containing some functional atoms or groups such as nitrogen, oxygen or sulphur will have a good inhibition effect[4-7]. Among these various inhibitors, benzimidazole and its derivatives[8-10] as corrosion inhibitors are arousing more attention owing to their special molecular structural with a five-membered ring containing nitrogen, where the ring connected with different substituent group. The inhibition performances of some different organic compounds, such as benzimidazole, 2-methylbenzimidazole

and 2-mercaptobenzimidazole have been investigated for mild steel in acid solution through some experimental methods [11].

The use of quantum chemical method is a good way to study the fundamental properties of molecular structure and their performance. This method is widely used to discuss the relationship between the structure and performance of corrosion inhibitors and studying corrosion inhibition at micro level [12-15]. Some related theoretical research was investigated for these benzimidazole inhibitors [16], but the detailed relationship between the quantum structural parameters and inhibition efficiency of these inhibitors were not fully investigated yet. The aim of this research will calculate the most relevant quantum parameters, explore their relationship with inhibition efficiency, and most importantly, based on structure-activity relationship studies then design some new homologous inhibitors with better inhibition performance. Hence, some quantum parameters are calculated, such as the highest occupied molecular orbital energy (E_{HOMO}), the lowest unoccupied molecular orbital energy (E_{LUMO}), energy gap (ΔE), the Mulliken charge distributions and so on. Based on these theoretical calculations, results are discussed using linear regression analysis method in order to find out which parameters may have a good linear relationship with inhibition efficiency, which will provide some useful information to design and discover new homologous benzimidazole inhibitors with better efficiency.

Table 1. Abbreviations and molecular structure of the studied inhibitors

Inhibitor	Conformation	Abbreviation
Benzimidazole		M1
2-Methylbenzimidazole		M2
2-Mercaptobenzimidazole		M3

2. CALCULATION METHODS

To search the optimized structures and calculate the quantum parameters of the inhibitors, DFT (density functional theory) methods were used in the study [17,18]. Calculations were performed at the DFT level using three basis sets, 6-31+G(d), 6-31G+(d,p) and 6-31+G(d,p) with B3LYP functional [19,20]. Making sure all the structures are optimized and verified without imaginative frequencies, after that we calculated these molecular parameters, namely the highest occupied molecular orbital energy (E_{HOMO}), the lowest unoccupied molecular orbital energy (E_{LUMO}), energy gap ($\Delta E = E_{LUMO} - E_{HOMO}$), and Mulliken charge distribution, etc. In addition, as for the effect of solvent, the theoretical model was considered via PCM [21], using a dielectric constant of 78.5 for water [22]. All the calculations were carried out by using the Gaussian09 software [23] on a personal computer.
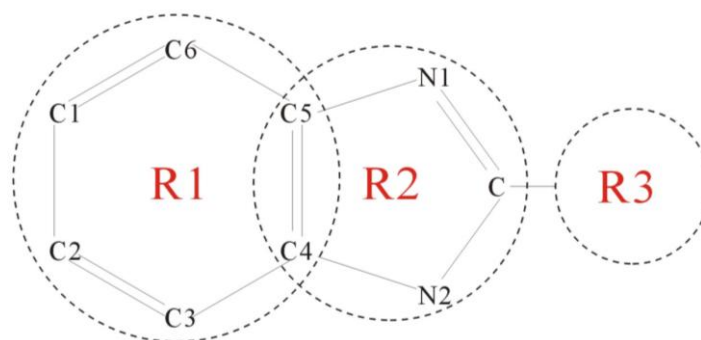
3. RESULTS AND DISCUSSION

Figure 1. The molecular schematic of inhibitor

The chemical structures and the atomic or group numbering scheme of inhibitor are presented in Fig.1. After using 6-31+G(d), 6-31+G(d,p) and 6-311+G(d,p) DFT methods, structural parameters such as E_{HOMO}, E_{LUMO}, $\Delta E = E_{HOMO} - E_{LUMO}$, and mulliken charges of some atoms or groups have been calculated and shown in Table 2, where R1, R2 represent the ring shown in Fig.1 and R3 is a various substituent. Q_{N1} and Q_{N2} refer to net charge of N1 and N2; Q_{R1} and Q_{R2} refers to net charge of ring R1 and R2; and Q_{R3} refers to the charge of R3.

Table 2. Calculated quantum chemical parameters of the studied inhibitors

Method	Inhibitor	E_{HOMO}	E_{LUMO}	ΔE	Q_{N1}	Q_{N2}	$Q_{(N1+N2)}$	Q_{R1}	Q_{R2}	Q_{R3}	IE[a]
B3LYP/6-31+G(d)	M1	-6.368	-0.762	-5.606	-0.499	-0.61	-1.109	-0.791	1.129	0.242	52.2
	M2	-6.204	-0.626	-5.578	-0.524	-0.639	-1.163	-0.989	1.944	-0.051	57.1
	M3	-6.095	-0.735	-5.361	-0.426	-0.576	-1.002	-1.196	1.917	0.177	88.8
B3LYP/6-31G+(d,p)	M1	-6.395	-0.762	-5.633	-0.487	-0.448	-0.935	-0.58	0.6	0.188	52.2
	M2	-6.232	-0.653	-5.578	-0.497	-0.452	-0.949	-0.832	1.03	0.169	57.1
	M3	-6.095	-0.762	-5.334	-0.403	-0.395	-0.798	-1.008	1.13	0.227	88.8
B3LYP/6-31+G(d,p)	M1	-6.449	-0.844	-5.606	-0.331	-0.267	-0.598	-0.841	0.953	0.179	52.2
	M2	-6.286	-0.708	-5.578	-0.297	-0.241	-0.538	-0.856	1.301	0.047	57.1
	M3	-6.150	-0.816	-5.334	-0.245	-0.184	-0.429	-0.843	2.041	-0.353	88.8

a Experimental values from Ref.[11] the inhibition efficiency (IE) for the corrosion of mild steel tested in 1M HCl solution with addition of 250 ppm of various inhibitors.

3.1 Correlation between molecular orbital energies and inhibition efficiency

According to the frontier molecular orbital theory [24], the interaction between reactants only happens in frontier molecular orbitals. In order to know the adsorption process of inhibitor we should take the HOMO and LUMO orbitals into consideration. The frontier orbitals of HOMO and LUMO of each inhibitor are shown in Fig.2, from which we can find that the three inhibitors have the same activity centers. The HOMO is largely located on the benzene ring (R1) and imidazole ring (R2). But the LUMO is spread more evenly on each molecule. The HOMO distribution is planar and makes the molecule be adsorbed on the metal surface perfectly, because it is easy for the empty orbital of metal to accept the electron provided by inhibitors.

Using linear fitting with corrosion inhibition efficiency (IE) and frontier orbital energy, we get these parameters such as regression equations and multiple correlation coefficients by using various basis sets, 6-31+G(d), 6-31G+(d,p) and 6-31+G(d,p). All these parameters are displayed in Table 3. The best correlation is observed with HOMO-LUMO energy gap no matter what the basis set is. That means lower absolute value of energy gap will give good inhibition efficiency because the energy needs to remove an electron from the frontier orbital (HOMO) will be lower than these higher energy gap [25].
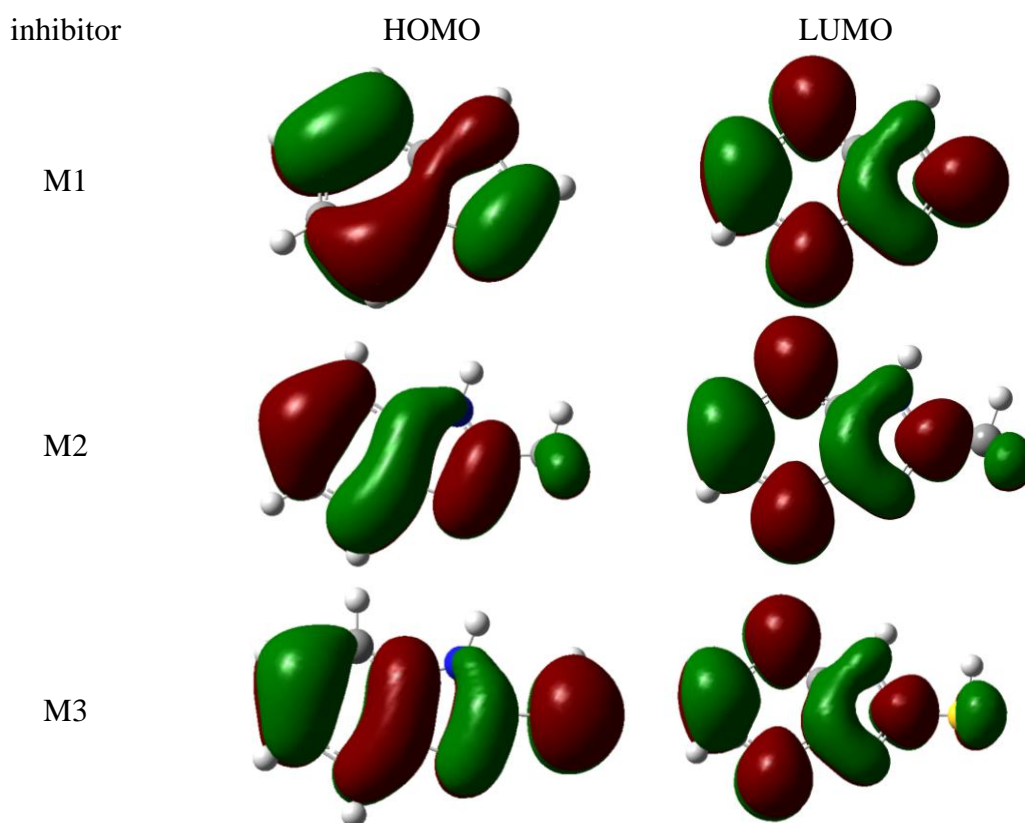

Figure 2. The frontier molecule orbital density distribution of three inhibitors after optimization using DFT B3LYP/6-31+G(d,p) method

Hence it is easy for the metal atom to accept the electron from the HOMO orbital of inhibitor with lower absolute energy gap. Another better correlation is observed with HOMO energy. From

Table 3, we can find that the inhibitor with lower absolute value of energy gap often has a higher HOMO energy which infers that the electron of HOMO may have higher activity. Higher HOMO energy indicates that the inhibitor has a tendency to provide electron to the metallic surface atom and the inhibition efficiency will increase too.

Table 3. The regression equations of corrosion inhibition efficiency and their frontier orbital energy

| Method	Variable	Regression equation		Multiple R	R Square
B3LYP/6-31+G(d)	E_{HOMO}	IE=848.627+125.772* E_{HOMO}	(1)	0.8699	0.7567
	E_{LUMO}	IE =25.067-57.889* E_{LUMO}	(2)	0.2098	0.0440
	ΔE	IE =882.979+148.132*ΔE	(3)	0.9998	0.9996
B3LYP/6-31G+(d,p)	E_{HOMO}	IE =809.428+119.121* E_{HOMO}	(4)	0.9005	0.8108
	E_{LUMO}	IE =-23.177-122.936* E_{LUMO}	(5)	0.3894	0.1516
	ΔE	IE =753.683+124.687*ΔE	(6)	0.9988	0.9975
B3LYP/6-311+G(d,p)	E_{HOMO}	IE =817.565+119.386* E_{HOMO}	(7)	0.8996	0.8092
	E_{LUMO}	IE =21.843-55.985* E_{LUMO}	(8)	0.2024	0.0409
	ΔE	IE =796.887+132.738*ΔE	(9)	0.9996	0.9991

3.2 Correlation between Mulliken charge and inhibition efficiency

Correlations are also investigated between the experimental corrosion inhibition parameters and the Mulliken charges of various atoms and groups by using various basic sets. We make the analysis on linear regression of net charges, such as Q_{N1}、 Q_{N2}、$Q_{(N1+N2)}$ 、Q_{R1}、Q_{R2} and Q_{R3}. The charge of N1 correlates best by using three methods. With the basic set changing from 6-31+G(d) to 6-311+G(d,p), the calculation accuracy increases. All the correlations are improved and group R3 seems to do the best with R=0.9932. This means the substituent chargeability play a critical influence on inhibition performance when inhibitor molecule with the same primary structure.

To further investigate which part of the inhibitor plays an important role on the efficiency during the surface adsorption, molecular electrostatic potential surface are calculated using DFT B3LYP/6-311+G(d,p) method. From Figure 3 it is easy to see that the negative charge centers mainly on the benzene ring and the imidazole ring atoms (N2). As for inhibitor C, there is a little negative charge on substituent −SH. Hence, we can infer that when the inhibitor adsorb on a surface benzene ring and imidazole ring (especially N2 atom) play a mainly role, but substituents also play a synergistic role which explains why the charge of R3 correlates best with inhibition efficiency.

Table 4. The regression equations of corrosion inhibition efficiency and different net charges

Method	Variable	Regression equation		Multiple R	R Square
B3LYP/6-31+G(d)	Q_{N1}	IE=241.621+363.536* Q_{N1}	(10)	0.9317	0.8681
	Q_{N2}	IE=382.069+519.511* Q_{N2}	(11)	0.8245	0.6798
	$Q_{(N1+N2)}$	IE=303.211+217.329* $Q_{(N1+N2)}$	(12)	0.8963	0.8034
	Q_{R1}	IE=85.439+38.426* Q_{R1}	(13)	0.5345	0.2857
	Q_{R2}	IE=24.669+24.869* Q_{R2}	(14)	0.5795	0.3358
	Q_{R3}	IE=63.086+24.025* Q_{R3}	(15)	0.1861	0.0346
B3LYP/6-31G+(d,p)	Q_{N1}	IE=239.645+375.513* Q_{N1}	(16)	0.9758	0.9521
	Q_{N2}	IE=330.911+613.615* Q_{N2}	(17)	0.9827	0.9656
	$Q_{(N1+N2)}$	IE=274.353+233.020* $Q_{(N1+N2)}$	(18)	0.9785	0.9575
	Q_{R1}	IE=98.995+77.495* Q_{R1}	(19)	0.6967	0.4853
	Q_{R2}	IE=18.322+51.860* Q_{R2}	(20)	0.7350	0.5403
	Q_{R3}	IE=-51.705+604.823* Q_{R3}	(21)	0.9001	0.8103
B3LYP/6-311+G(d,p)	Q_{N1}	IE=194.331+440.885* Q_{N1}	(22)	0.9611	0.9238
	Q_{N2}	IE=172.090+459.784* Q_{N2}	(23)	0.9825	0.9652
	$Q_{(N1+N2)}$	IE=183.707+225.573* $Q_{(N1+N2)}$	(24)	0.9727	0.9462
	Q_{R1}	IE=77.235+74.510* Q_{R1}	(25)	0.9842	0.9686
	Q_{R2}	IE=15.810+35.080* Q_{R2}	(26)	0.9811	0.9625
	Q_{R3}	IE=63.018-71.231* Q_{R3}	(27)	0.9932	0.9864

M1   M2   M3
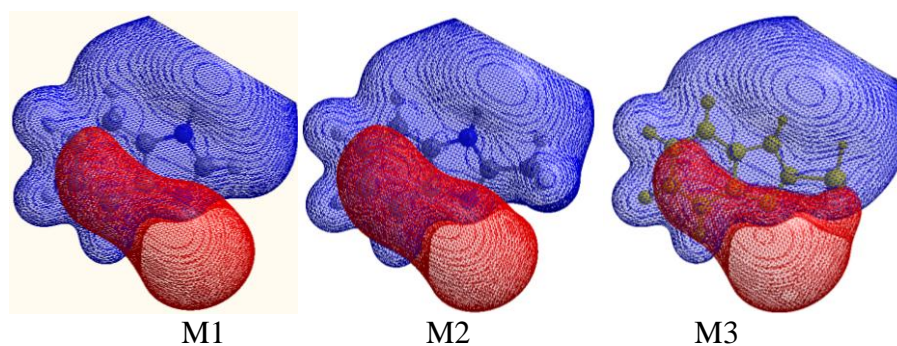
Figure 3. The molecular electrostatic potential surface of three inhibitors (using DFT B3LYP/6-311+G(d,p) method) with isopotential value of 0.8 a.u. Negative regions are shown in red, positive in blue

3.3 Prediction of the efficiency of some new inhibitors

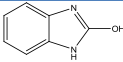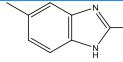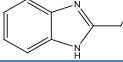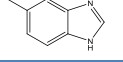**Table 5.** Structure of some kinds of homologous inhibitors
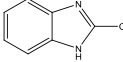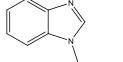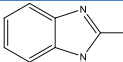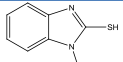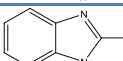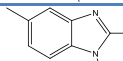
Inhibitors	Conformations	Inhibitors	Conformations
M4		M9	
M5		M10	
M6		M11	
M7		M12	
M8		M13	

Table 6. Calculated quantum chemical parameters and prediction of inhibition efficiency for homologous inhibitors

Inhibitor	HOMO/ev	LUMO/ev	ΔE/ev	Q_{R3}	Prediction of inhibition efficiency			Average
					IE=817.565+119.386*E_{HOMO}	IE=796.887+132.738*ΔE	IE=63.018-71.231*Q_{R3}	
M4	-6.193	-0.571	-5.622	-0.015	78.21	50.58	64.09	64.29
M5	-6.318	-0.715	-5.603	0.108	63.28	53.18	55.33	57.26
M6	-6.138	-0.565	-5.573	0.048	84.77	57.12	59.60	67.16
M7	-6.405	-0.869	-5.535	0.071	52.90	62.14	57.96	57.67
M8	-6.322	-0.777	-5.545	-0.097	62.81	60.91	69.93	64.55
M9	-6.042	-0.764	-5.278	-0.389	96.23	96.28	90.73	94.41
M10	-6.294	-0.783	-5.511	-0.085	66.15	65.32	69.07	66.85
M11	-6.367	-0.799	-5.568	0.269	57.43	57.74	43.86	53.01
M12	-6.132	-0.820	-5.312	-0.218	85.49	91.83	78.55	85.29
M13	-6.000	-0.756	-5.244	-0.300	101.25	100.75	84.39	95.46

From previous study we found that the main structure of these inhibitors played an important role on the inhibition efficiency. In order to play a better performance the main structure should contain R1 and R2. So we can design some other homologous corrosion inhibitors just change some substituent group of R1 and R2 (Table 6), then obtain their quantum chemical parameters using B3LYP/6-311G(d,p) method and predict their inhibition efficiency using the formula (7), (9) and (27) (presented in Table 3 and Table 4).

It is easy to find from table 6 that M9 and M13 have a better performance. In order to illustrate why these inhibitors have a better performance, the fraction of electrons transferred from inhibitors to metal (ΔN) such as iron have been calculated and it has the following format [26-30]: $\Delta N=(\chi_{Fe}-\chi_{inh})/2(\eta_{Fe}+\eta_{inh})$, where χ_{Fe} and χ_{inh} represent the absolute electro-negativity of iron and the inhibitor respectively, η_{Fe} and η_{inh} represent the absolute hardness of iron and the inhibitor. As for inhibitor, (χ) and global hardness (η) [31] are calculated as: $\chi=(I+A)/2$, $\eta=(I-A)/2$. ionization potential (I) and

electron affinity (*A*) are related to the energy of HOMO and LUMO orbitals where: $I = -E_{HOMO}$ and $A = -E_{LUMO}$.[26]. As for iron, we use a theoretical value, $\chi_{Fe} = 7.0$ev/mol and $\eta_{Fe} = 0$ ev/mol according to assumption that as for a metallic bul*k, I=A*, because they are softer than neutral metallic atoms [31]. Hence, we calculated all the fraction of electrons transferred from inhibitor to the iron surface (ΔN). According to some research [26,27], the values of ΔN indicate inhibition performance results from electrons donation. Some study [27] suggested that if $\Delta N < 3.6$, the inhibition efficiency increased with enhancing electron donation ability on a metal surface. From Table 7, it is very easy to find that M9 and M13 have more electrons transferred to iron surface, so they have better corrosion performance which is also consistent with the results in Table 6.

Table 7. The fraction of electrons transferred from inhibitor to the iron surface (ΔN).

Inhibitor	HOMO/ev	LUMO/ev	ΔE/ev	χ	η	ΔN
M1	-6.449	-0.844	-5.606	3.6465	2.8025	0.59831
M2	-6.286	-0.708	-5.578	3.497	2.789	0.62800
M3	-6.150	-0.816	-5.334	3.483	2.667	0.65936
M4	-6.193	-0.571	-5.622	3.382	2.811	0.64354
M5	-6.318	-0.715	-5.603	3.5165	2.8015	0.62172
M6	-6.138	-0.565	-5.573	3.3515	2.7865	0.65467
M7	-6.405	-0.869	-5.535	3.637	2.768	0.60748
M8	-6.322	-0.777	-5.545	3.5495	2.7725	0.62227
M9	-6.042	-0.764	-5.278	3.403	2.639	0.68151
M10	-6.294	-0.783	-5.511	3.5385	2.7555	0.62811
M11	-6.367	-0.799	-5.568	3.583	2.784	0.61369
M12	-6.132	-0.82	-5.312	3.476	2.656	0.66340
M13	-6.000	-0.756	-5.244	3.378	2.622	0.69069

4. CONCLUSIONS

Through quantum chemical calculations at the DFT level using three basis sets, 6-31+G(d), 6-31G+(d,p) and 6-311+G(d,p) with B3LYP functional for three kinds of benzimidazole inhibitors compounds, some quantum parameters such as highest occupied molecular orbital (HOMO), lowest unoccupied molecular orbital (LUMO), energy gap between HOMO & LUMO and Mulliken charges have been obtained. The relationship between the corrosion inhibitor efficiency and chemical quantum parameters are discussed by using linear regression analysis. The results show that the inhibition efficiency enhances with the increase of E_{HOMO} and ΔE, and the efficiency correlates best with ΔE. We calculate the Mulliken charges with different basic sets and the results show that correlation seems best with basic set 6-311+G(d,p) which may provide more accurate calculation result. All the correlations are improved using basic set 6-311+G(d,p) and charges of group R3 seems to do the best correlation with R=0.9932. This means the substituent charge ability may play a critical influence on inhibition performance when inhibitor molecule with the same primary structure.

Based on this information, we have attempted to design some new homologous molecules, calculate their quantum chemical structure parameters and predict their performance. It is hope the testing will help to design some inhibitor molecules with good performance.

References

1. S.A. Abd El-Maksoud, A.S. Fouda, *Mater. Chem. Phys.* 93 (2005) 84.
2. M. Benabdellah, R.Touzani, A.Aouniti, A. Dafali, S. Elkadiri, B. Hammouti and M. Benkaddour , *Phys. Chem. News* 37(2007) 63.
3. L. Wang, *Corros. Sci.* 43 (2001) 2281.
4. J.Hong, Z.P. Kai, L.Yan, *Corros. Sci.* 50 (2008) 865.
5. K.F. Khaled, *Corros. Sci.* 52 (2010) 2905.
6. I. B. Obot, N. O. Egbedi, *Corros. Sci.* 52 (2010) 282.
7. G. Gao, C.H. Liang, H. Wang, *Corros. Sci.* 49 (2007) 1833.
8. K. Laarej, M. Bouachrine, S. Radi, S. Kertit, B. Hammouti, *E-J. Chem.* 7 (2010) 419.
9. O. Benali, L. Larabi, M. Traisnel, L. Gengembra, Y. Harek, *Appl. Surf. Sci.* 253 (2007) 6130.
10. K.F. Khaled, *Electrochim. Acta*, 48 (2003) 2493.
11. J. Aljourani, K. Raeissi, M.A. Golozar, *Corros. Sci.* 51 (2009) 1836.
12. G. Gece, S. Bilgiç, *Corros. Sci.* 52 (2010) 3435.
13. S.K. Chen, T. Kar, *Int. J. Electrochem. Sci.* 7 (2012) 6265.
14. S.K. Chen, S. Scheiner, T. Kar, U. Adhikari, *Int. J. Electrochem. Sci.* 7(2012) 7128.
15. J.F. Zhu, S.K. Chen, *Int. J. Electrochem. Sci.*7 (2012) 11884.
16. I.B. Obot, N. O. Egbedi, *Corros. Sci.* 52 (2010) 657.
17. P. Hohenberg, W. Kohn, *Phys. Rev*. 136 (1964) B864.
18. W. Kohn, L. J. Sham, *Phys. Rev.* 140 (1965) A1133.
19. A.D. Becke, *J. Chem. Phys.* 98 (1993) 5648.
20. C. Lee, W. Yang, R.G. Parr, *Phys. Rev. B* 37 (1998) 85.
21. J. Tomasi, B. Mennucci, R. Cammi, *Chem. Rev.* 105 (2005) 2999.
22. A. V. Marenich, C. J. Cramer, D. G. Truhlar, *J. Phys. Chem.* B 113 (2009) 6378
23. M. J. Frisch, G .W. Trucks, H. B. Schlegel, Gaussian , revision B 09 Pittsburgh, Pa: Gaussian Inc, 2009
24. K. Fukui, Theory of Orientation and Stereoselection, Springer-Verlag, New York, 1975.
25. G. Gece, *Corros. Sci.* 50 (2008) 2981.
26. V.S. Sastri, J.R. Perumareddi, *Corros.* 53 (1997) 617.
27. I. Lukovits, E. Kalman, F. Zucchi, *Corrosion* 57 (2001) 3.
28. S. Martınez, *Mater. Chem. Phys*. 77 (2002) 97.
29. J.C. Slater, Introduction to Chemical Physics, Dover, New York, 1970.
30. M.J.S. Dewar, W. Thiel, *J. Am. Chem. Soc.* 99 (1977) 4899.
31. R.G. Pearson, *Inorg. Chem.* 27 (1988) 734.